

Integration of Network Pharmacology, Molecular Docking, and Molecular Dynamics to Evaluate *Calotropis gigantea* flowers Bioactive Compounds as Anti-Cervical Cancer Agents

Suresh Kumar Gopal^{*1}, Rakesh Kumar Jat², Abdul Mannan Khan³

¹Research Scholar, Department of Pharmaceutical Sciences, Shri Jagdishprasad Jhabarmal Tibrewala University, Vidyanagari, Jhunjhunu Churu Road, Chudela, District - Jhunjhunu Rajasthan – 333010. Mobile no: 9384266716; e-mail ID: Sureshbiotech1983@gmail.com. ORCID ID: 0009-0004-5034-0166

²Director-cum-Principal, Department of Pharmacy, Shri Jagdishprasad Jhabarmal Tibrewala University, Vidyanagari, Jhunjhunu Churu Road, Chudela, District - Jhunjhunu Rajasthan – 333010. Mobile no: 9667212243; e-mail ID: pharmacy@ijtu.ac.in

³Professor, Department of Pharmacy, Shri Jagdishprasad Jhabarmal Tibrewala University, Vidyanagari, Jhunjhunu Churu Road, Chudela, District - Jhunjhunu Rajasthan – 333010. Mobile no: 9571063360; e-mail ID - drmannan.bux@gmail.com

Abstract

Cervical cancer remains the fourth most prevalent malignancy among women worldwide, presenting a severe health burden particularly in low-resource regions where therapeutic options are limited. This study investigates the anti-cervical cancer potential of bioactive compounds from *Calotropis gigantea* flowers using an integrated pipeline of network pharmacology, molecular docking, and molecular dynamics simulations. Phytochemical screening identified 31 compounds, which were subjected to ADME profiling; flavonoids such as quercetin and kaempferol exhibited superior drug-likeness and oral bioavailability compared to high-molecular-weight cardenolides.

A systems-level analysis identified 571 common targets between *C. gigantea* bioactives and cervical cancer. Through protein–protein interaction network analysis, AKT1, EGFR, SRC, and STAT3 were identified as the primary hub genes governing tumor progression. Functional enrichment results indicated that these targets are central to the PI3K-AKT and EGFR-tyrosine kinase inhibitor resistance pathways. Survival analysis further highlighted JUN (HR = 1.7) and EGFR (HR = 1.6) as significant prognostic biomarkers for poor clinical outcomes in cervical cancer patients.

Molecular docking simulations explored the binding orientations of these ligands within the active sites of key proteins. In this study, quercetin and kaempferol demonstrated potent binding affinities for SRC (–9.10 kcal/mol and –8.80 kcal/mol, respectively) and EGFR (–8.90 kcal/mol), interacting with critical residues such as MET-793 and THR-338. Subsequent MD simulations validated the structural stability of these complexes. Notably, the quercetin–SRC complex exhibited a remarkably low eigenvalue (9.14973×10^{-5}) and stabilized fluctuation profiles, indicating high energetic favorability and structural integrity over time. These results suggest that *C. gigantea* flower bioactives, particularly quercetin and kaempferol, are promising multi-targeted candidates for further therapeutic development.

Keywords: *Calotropis gigantea*, Cervical Cancer, Network Pharmacology, Molecular Docking, Molecular Dynamics, Quercetin, Kaempferol, AKT1, SRC, Hub Genes.

1. Introduction

Cervical cancer remains a significant global health challenge, ranking as the fourth most common cancer among women worldwide, with an estimated 604,000 new cases recorded in 2020 (2,13). Despite the implementation of human papillomavirus vaccinations and screening programs, it continues to be a leading cause of mortality for women in low- and middle-income countries where access to healthcare infrastructure is limited (1,2). Current standard therapies, including surgical intervention, chemotherapy, and radiotherapy, often face substantial hurdles such as systemic toxicity, the development of drug resistance, and poor prognosis for advanced or metastatic stages, where the 5-year survival rate drops to approximately 19% (1,2). Consequently, there is an urgent demand for the development of novel, effective, and affordable antineoplastic medications (14).

Natural products derived from medicinal plants have historically played a vital role in drug discovery, offering a diverse library of bioactive secondary metabolites with potent inhibitory effects against various cancer types (14,15). Among these, *Calotropis gigantea* Dryand, a member of the Apocynaceae family, has garnered significant attention for its wide-ranging pharmacological properties (12). Phytochemical investigations have identified several classes of bioactive compounds within the plant, including alkaloids, flavonoids, terpenoids, and cardiac glycosides such as cardenolides (12,16). Specifically, cardenolides like calotropin and uscharin isolated from *C. gigantea* have demonstrated cytotoxic activity against various human cancer cell lines, including breast, colon, and cervical cancer cells (16–18). While much research has focused on the roots and leaves, the flowers of *C. gigantea* also possess significant antitumor potential, yet their specific molecular mechanisms against cervical cancer remain to be fully elucidated (11).

Traditional drug discovery methods are often time-consuming, expensive, and labor-intensive (14). To overcome these limitations, modern computational approaches such as network pharmacology and molecular docking have emerged as powerful tools for identifying therapeutic targets and predicting the efficacy of plant-based compounds(14,19) Network pharmacology adopts a holistic "multi-target, multi-pathway" approach, allowing researchers to map phytochemicals to specific signaling pathways (e.g., KEGG or Reactome) and construct drug-target-disease networks(19,20) Complementing this, molecular docking provides a structural basis for these interactions by simulating the binding affinity of phytochemicals to key cancer-associated proteins(15,21)

This study aims to decipher the anticancer arsenal of *Calotropis gigantea* flowers by integrating network pharmacology and molecular docking. By identifying the core phytochemical targets and the underlying signaling pathways involved in cervical cancer progression, this research seeks to provide a scientific foundation for the development of new, targeted therapies derived from this ethnomedicinal resource.

2.Methodology

2.1 Identification of bioactive compounds present in *Calotropis gigantea* flowers

Bioactive compounds present in the flowers of *Calotropis gigantea* through literature mining (12,16), coupled with the utilization of the IMPPAT database (<https://cb.imsc.res.in/imppat/>) with "*Calotropis gigantea*" as keywords (22,23). All compounds and their canonical sequences were retrieved from PubChem (<https://pubchem.ncbi.nlm.nih.gov/>) (24,25).

2.2 Identification of potential compounds present in *Calotropis gigantea* flowers

The bioactive compounds identified in the earlier step underwent ADME analysis using the SwissADME server (<http://www.swissadme.ch/>) (3). SwissADME was used to evaluate the pharmacokinetic properties, drug-likeness, and medicinal chemistry compatibility of the small compounds (3,4). ADME, an abbreviation in pharmacokinetics, encompasses the processes of absorption, distribution, metabolism, and excretion, playing a pivotal role in drug discovery (4,26). Oral bioavailability is a critical pharmacokinetic measure that indicates a drug's capacity to enter systemic circulation following oral delivery (26). Drug-likeness refers to the similarity between a chemical and existing medication (3). OB and DL were used as the primary parameters for screening the active constituents (15,21). To adhere to the ADME criteria, specific restrictions were imposed, such as an overall OB $\geq 30\%$ (15,21) and the exclusion of violations pertaining to Lipinski's rule of 5, to filter the phytochemical components (3,26).

2.3 Identification of potential targets of *C.gigantea* flowers

Target interactions of the bioactive compounds were investigated using SwissTargetPrediction (<http://www.swisstargetprediction.ch/>) (27). Target selection was conducted using the SwissTargetPrediction tool with a p-value greater than 0.4 (28). This systematic target mapping approach enables the identification of molecular interactions specific to the phytochemical profile of *C.gigantea* flowers.

2.4 Screening for disease targets for Cervical cancer

Various databases, including the Therapeutic Target Database (<https://db.idrblab.net/ttd/>) (8), OMIM (<https://www.omim.org/>) (with a probability threshold > 0.4) (5,29), and GeneCards (<https://www.genecards.org/>) (with a relevance score exceeding 30) (5,30), have been used to identify the target proteins associated with cervical cancer (5,8,30).

2.5. Identification of Overlapping Drug-Disease Targets

Common targets between the identified floral phytochemicals and cervical cancer-associated proteins were identified using the Venny 2.1.0 web tool (<https://bioinfo.gp.cnb.csic.es/tools/venny/>) (5,30). The intersection of these target sets reveals core therapeutic targets through which the bioactive constituents of *Calotropis gigantea* flowers potentially exert their antineoplastic effects (5,8). This comparative analysis is essential for visualizing the drug-disease target overlap, providing critical insights into the multi-target mechanism of action and the complex relationships between bioactive substances and their corresponding molecular pathways in cervical cancer (5,30).

2.5. Protein-Protein Interaction Network Construction and Topological Analysis

Protein-protein interactions are fundamental to governing cellular functions and complex biological processes, providing a systems-level understanding of infection mechanisms and facilitating the development of targeted therapeutic strategies (31,32). To elucidate the functional crosstalk between the identified targets of *Calotropis gigantea* floral phytochemicals and cervical cancer-associated proteins, a PPI network was constructed using the STRING database (<https://string-db.org/>) (5,33). The analysis was restricted to *Homo sapiens* with a high-confidence interaction score threshold of 0.7 to ensure the reliability of the predicted and experimental associations (10,34). The resulting interaction data were exported in a tab-separated value format and imported into Cytoscape v3.9.1 software for advanced visualization and network analysis (35,36). Topological parameters, including degree centrality, betweenness centrality, and closeness centrality, were calculated to identify pivotal hub genes within the network, while functional enrichment was performed to map these interactions to specific Gene Ontology terms and KEGG signaling pathways (6,36,37).

2.6. Construction and Topological Analysis of the Compound–Target–Disease (C–T–D) Network

A Compound–Target–Disease (C–T–D) network was constructed to visualize the complex multi-component and multi-target mechanisms of *Calotropis gigantea* floral phytochemicals against cervical cancer using Cytoscape v3.9.1 software (<https://cytoscape.org/>) (10,36). The network integrated distinct nodes representing the identified bioactive compounds, their corresponding protein targets, and the disease state (5,34). To quantify the significance of each node within the biological system, network topology was analyzed using the CytoHubba plugin, which calculated centrality measures such as degree, betweenness, and closeness (35,37). Advanced visualization techniques, including color and node-size scaling, were employed to depict the architecture; the diameter of each node was mapped to its degree of connectivity, ensuring that the largest nodes represented the most critical hub components or targets with the highest number of interactions (6,36). Finally, the phytochemical components were ranked in ascending order of importance based on their degree values to prioritize candidate molecules for further mechanistic validation (33,37).

2.7. Functional Enrichment and Pathway Analysis

Functional and biological pathway enrichment analysis was performed using ShinyGO 0.7 (<http://bioinformatics.sdstate.edu/go/>) to elucidate the molecular mechanisms governing the identified target genes (6,30). This platform incorporates a comprehensive set of enrichment ontologies, including Gene Ontology biological processes, Kyoto Encyclopedia of Genes and Genomes pathways, Reactome gene sets, canonical pathways, and the Comprehensive Resource of Mammalian Protein Complexes (34,36). Specifically, GO biological process enrichment and KEGG pathway analysis were applied to the core targets identified within the protein–protein interaction network to identify the signaling cascades modulated by *Calotropis gigantea* floral phytochemicals in the context of cervical cancer (5,8,10). This systematic annotation enables the identification of critical regulatory pathways—such as those involved in cell cycle control and apoptosis—that are pivotal to the antineoplastic activity of these bioactive compounds (30,34).

2.8. Validation of Hub Gene Expression via GEPIA 2

The Gene Expression Profiling Interactive Analysis (GEPIA 2, <http://gepia.cancer-pku.cn/>) database was utilized to evaluate the expression profiles of the identified hub genes within clinical datasets (8,34). Specifically, the mRNA expression levels of these core targets were compared between Cervical Squamous Cell Carcinoma and Endocervical Adenocarcinoma samples and corresponding normal tissues (34). Following the criteria established by Muthuramalingam et al., the thresholds for significant differential expression were set at a $|\log_2FC|$ value of 1 and a p-value of 0.01 (30,34). This validation step confirms the clinical relevance of the predicted targets, ensuring they are significantly dysregulated in cervical cancer patients and reinforcing their potential as viable therapeutic targets for *Calotropis gigantea* floral phytochemicals (8,34).

2.9. Prognostic Value and Survival Analysis

Overall survival and survival map analysis of the top five identified hub genes were conducted to evaluate their prognostic significance in cervical cancer using the GEPIA 2 server (8,34). The expression-based survival impact was validated against the built-in Cervical Squamous Cell Carcinoma and Endocervical Adenocarcinoma datasets to predict how these molecular targets influence patient survival time (34). Survival curves were generated using the Kaplan-Meier plotter within GEPIA 2, employing preset default parameters to determine the correlation between high and low gene expression levels and clinical outcomes (30,34). This analysis is critical for confirming that the predicted targets of *Calotropis gigantea* floral phytochemicals are not only differentially expressed but also serve as reliable prognostic biomarkers for cervical cancer progression (8,34).

2.10. Molecular Docking and Binding Affinity Analysis

Molecular docking studies were performed to elucidate the binding mechanisms and orientations of *Calotropis gigantea* floral phytochemicals within the active sites of identified cervical cancer targets (30,34). The 3D structures of the target proteins were retrieved and visualized using UCSF Chimera, which served as the primary platform for structural preparation (38). Both the preparation of the macromolecular targets and the energy minimization of the floral phytochemical ligands were conducted within the UCSF Chimera environment to ensure stable, low-energy conformations prior to docking (9).

The docking procedure was executed using the AutoDock Vina plugin integrated within UCSF Chimera (9). This computational approach explores various ligand conformations within the macromolecular binding sites to provide an accurate estimation of receptor–ligand binding free energies (9,38). AutoDock Vina is recognized for its high accuracy and computational efficiency in modern drug discovery workflows (9). Following the docking simulations, the resulting complexes and their intermolecular interactions were analyzed and visualized using BIOVIA Discovery Studio to evaluate the binding geometries and identify critical residues involved in the stabilization of the drug–target complexes (6,9). This multi-step process provides mechanical insights into how bioactive compounds potentially modulate core proteins involved in cervical cancer progression (6,34).

2.11. Molecular Dynamics Simulations

To further examine the dynamic behavior and stability of the docked complexes, molecular dynamics simulations were conducted using the iMODS platform (<https://imods.iqf.csic.es/>) (34). This tool utilizes Normal Mode Analysis to simulate biomolecular systems at the atomic level, providing essential insights into conformational changes, structural flexibility, and the stability of interactions over time (34).

In this investigation, MD simulations were performed on specific protein–ligand complexes, such as quercetin bound to five critical hub proteins—AKT1, EGFR, SRC, MMP9, and IGF1R—which are central to the pathophysiology of cervical cancer. The complexes were previously optimized through molecular docking to prepare them for dynamic analysis. Simulations were run for a duration of ten minutes using the default iMODS parameters, ensuring a standardized protocol that includes force field selection and integration time steps (34). This duration effectively captures critical molecular transitions and interactions that impact binding affinity. Furthermore, the CABS-flex 2.0 server (<https://biocomp.chem.uw.edu.pl/CABSflex2>) was employed to visualize the Root Mean Square Fluctuation values and generate contact maps, enabling the assessment of rigidity and stability within the protein–ligand complexes (10,34).

Results

3.1 Physicochemical and ADME Analysis of Bioactive Compounds from *Calotropis gigantea* flowers

A total of 31 bioactive compounds were examined for their drug-likeness and oral bioavailability using Lipinski's rule of five and SwissADME parameters, including molecular weight, hydrogen bond acceptors and donors, lipophilicity (MlogP), bioavailability score, and topological polar surface area (TPSA), are presented in Table 3.1. The investigation revealed that several compounds, specifically low-molecular-weight flavonoids and small heterocyclic compounds, exhibited favorable physicochemical properties with no Lipinski violations. Compounds such as flavylium, kaempferol, quercetin, caloside H, 5-hydroxy-(2-methoxymethyl) pyridine, nicotinic acid, p-(acetylamino)phenol, thymine, and 4'-methyl-2-phenylindole possessed molecular weights below 500 Da, acceptable hydrogen-bonding capacity, balanced lipophilicity, and TPSA values below 140 Å², indicating good potential for oral absorption and membrane permeability. By comparison, high-molecular-weight compounds such as uscharin, asclepin, calotropin, calactin, calotoxin, and cosmomycin B showed one or more Lipinski violations, primarily due to excessive molecular weight and/or high TPSA, which may impede gastrointestinal absorption. Highly lipophilic compounds, including β-amyryn, taraxasterol acetate, stigmasterol, and long-chain hydrocarbons, displayed increased MLogP values, indicating poor aqueous solubility irrespective of acceptable bioavailability scores. Most compounds showed a moderate predicted bioavailability score of 0.55, whereas nicotinic acid displayed an increased score (0.85), indicating superior oral bioavailability. Glutathione and cosmomycin B showed poor bioavailability due to their high polarity and molecular complexity. Overall, the Swiss ADME evaluation emphasized a subset of bioactive compounds with favourable drug-like properties appropriate for pharmacokinetic and molecular docking studies, whereas larger and highly lipophilic molecules may require structural optimization or alternative delivery methods.

Table 3.1: ADME properties of the selected bioactive compounds of *Calotropis gigantea* flowers

S.No	Nam of the compound	Lipinski Rules				Lipinski's Violations	Bioavailability Score	TPSA (Å ²)
		MW g/mol	HBA	HBD	MLog P			
		<500	<10	≤5	≤4.15	≤1	>0.1	<140
1	Uscharin	587.72	9	2	2.5	1	0.55	149.18
2	Flavylium	207.25	1	0	2.64	0	0.55	13.14
3	Asclepin	574.66	10	2	2.29	1	0.55	137.82
4	Calotropin	532.62	9	3	1.89	1	0.55	131.75
5	Calactin	532.62	9	3	1.89	1	0.55	131.75
6	Kaempferol	286.24	6	4	1.58	0	0.55	111.13
7	Quercetin	302.24	7	5	1.23	0	0.55	131.36
8	Calotoxin	548.62	10	4	1.01	0	0.55	151.98
9	Taraxasterol acetate	468.75	2	0	7.51	1	0.55	26.30

10	Beta-Amyrin	426.72	1	1	7.16	1	0.55	20.23
11	Glutathione	307.32	7	5	-2.36	0	0.11	197.62
12	Stigmasterol	412.69	1	1	6.98	0	0.55	20.23
13	Caloside H	338.31	8	4	-0.05	0	0.56	125.68
14	5-hydroxy-(2-methoxymethyl)pyridine	139.15	3	1	0.6	0	0.55	42.35
15	Nicotinic Acid	123.11	3	1	0.32	0	0.85	50.19
16	p-(acetylamino)phenol	151.16	2	2	0.93	0	0.55	49.33
17	Thymine	126.11	2	2	0.15	0	0.55	65.72
18	1-Tetradecene	196.37	0	0	5.71	1	0.55	0.00
19	3-Ethyl-1-Tetradecene	238.45	0	0	6.58	1	0.55	0.00
20	3-Octadecene, (E)	252.48	0	0	6.97	1	0.55	0.00
21	Pentadecanoic acid, 14-methyl-, methyl ester	270.45	2	0	5.48	1	0.55	26.30
22	9,12-Octadecadienoic acid, methyl ester	294.47	2	0	0	0	0	26.30
23	Ethyl linoleate	308.50	2	0	0	0	0	26.30
24	Methyl 17-methyl-octadecanoate	312.53	2	0	6.54	1	0.55	26.30
25	Docosane	310.60	0	0	8.64	1	0.55	0.00
26	Nonacosane	408.79	0	0	11.18	1	0.55	0.00
27	Tricosane	324.63	0	0	9	1	0.55	0.00
28	4' Methyl-2 Phenylindole	233.31	0	0	3.91	0	0.55	3.24
29	Heptacosane	380.73	0	0	10.46	1	0.55	0.00
30	Octadecane, 3-ethyl-5-(2-ethylbutyl)	366.71	0	0	9.68	1	0.55	0.00
31	Cosmomycin B	771.85	15	6	2.43	3	0.17	214.14

3.2 Prediction of potential targets for *Calotropis gigantea* flowers in the treatment of Cervical Cancer

Bioactive compounds from *Calotropis gigantea* flowers were subjected to target prediction analysis using SwissTargetPrediction, which identified 627 potential targets. A comprehensive analysis was conducted to identify the target genes associated with cervical cancer. By searching databases such as GEO Omnibus (GSE9750, GSE138080, and GSE7803), Malacards, OMIM, and GeneCards, with the keyword 'Cervical Cancer,' a total of 15824 target genes were retrieved. Using Venny 2.1.0, an overlap analysis between *Calotropis gigantea* flower-associated and cervical cancer-related targets identified 571 common targets (Fig. 3.1).

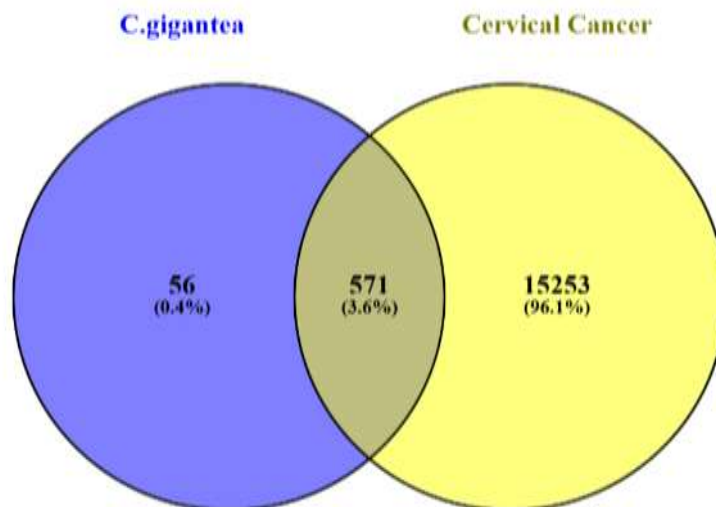


Fig. 3.1. Venn diagram illustrating the overlap between predicted targets of *Calotropis gigantea* flower-derived bioactive compounds and cervical cancer-associated genes.

3.3 Construction of Protein-Protein Network

Protein-protein interaction network analysis was performed using the STRING database, and the results are shown in Fig. 3.2. The proteins identified in the PPI network are represented by circular nodes, with their respective 3D structures depicted within the nodes. Protein interactions, shown as lines between nodes, have an increased number correlating with stronger interactions. Topological analysis was performed to identify the top 10 genes using the CytoHubba plug-in in Cytoscape 3.9. The top 10 identified genes were AKT1, ALB, SRC, EGFR, STAT3, ESR1, BCL2, CASP3, JUN, and HSP90AA1, as shown in Table 3.2. The top 10 PPI networks comprised 10 nodes and 45 edges, with an average of 188 neighbours. These hub genes, considered key regulatory genes, play a significant role in the treatment of cervical cancer, as shown in Fig. 3.3. Node scores are displayed by colour grading, with darker and redder nodes indicating higher node scores.

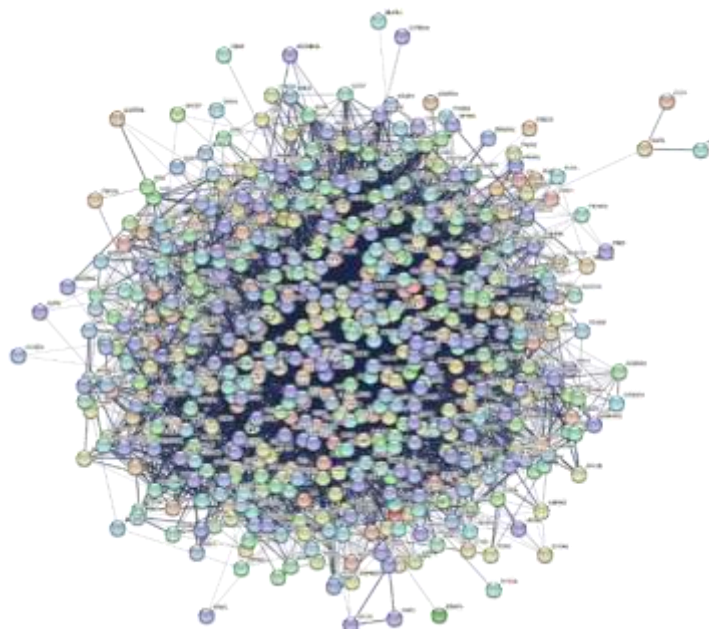


Fig. 3.2. Protein-protein interaction (PPI) network of potential targets for *Calotropis gigantea* flowers in the treatment of Cervical Cancer (CC)

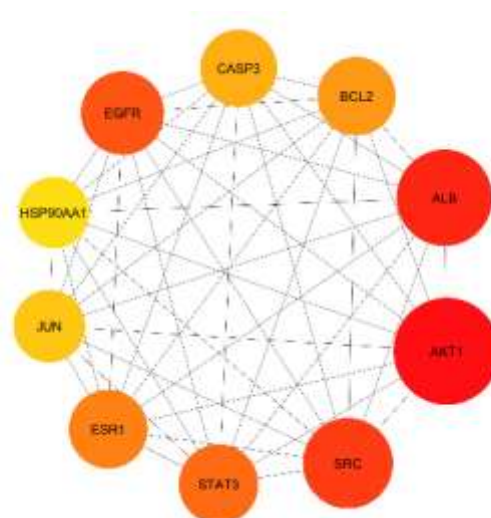


Fig. 3.3. Identification and ranking of Key Hub Genes in the Network Module Using CytoHubba in Cytoscape

Table 3.2: The degree centrality (DC), betweenness centrality (BC), and closeness centrality (CC) values of the hub genes

Gene	Degree	Betweenness	Closeness
AKT1	241	0.06034791	0.625962596
ALB	217	0.074424824	0.610515021
SRC	204	0.065718882	0.589026915
EGFR	188	0.037112487	0.587809917
STAT3	180	0.024100554	0.586597938
ESR1	178	0.039063151	0.578840285
BCL2	177	0.017946479	0.579429735
CASP3	174	0.020373998	0.576494428
JUN	163	0.01376423	0.56956957
HSP90AA1	161	0.021911324	0.563924678

3.4 C-T-D Network Construction and Analysis

3.4.1 Construction Compound Target Network

Cytoscape was used to construct a compound-target-pathway network to visualize the interrelationship between compounds, targets, and disease pathways. The C-T-D network is shown in Fig. 3.4. It consists of 91 nodes and 163 edges, with an average number of neighbours of 2.3. Table 3.3 displays the degree, betweenness, and closeness centralities of the top five bioactive compounds associated with cervical cancer. Among the bioactive compounds analysed, p-(acetylamino)phenol, kaempferol, 5-hydroxy-(2-methoxymethyl)pyridine, quercetin, and thymine showed the highest degrees, in the range of 3-5.

Table 3.3: Degree centrality (DC), betweenness centrality (BC), and closeness centrality (CC) values of compounds exhibiting high node degrees.

Compounds	Degree	Betweenness Centrality	Closeness Centrality
p-(acetylamino)phenol	5	0.28846286	0.458333333
Kaempferol	4	0.085830475	0.423076923
5-hydroxy-(2-methoxymethyl)pyridine	4	0.157363368	0.458333333
Quercetin	3	0.046327842	0.392857143
Thymine	3	0.135261708	0.423076923

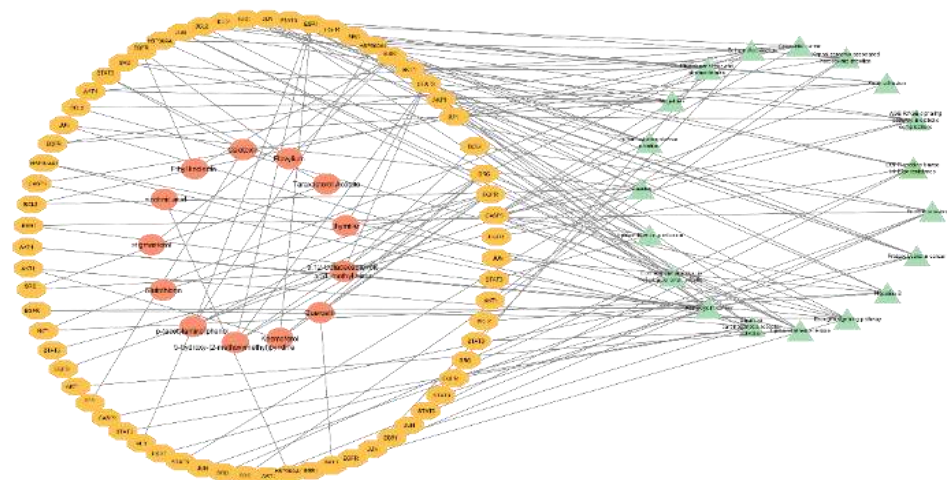


Fig. 3.4. Compound-target-pathway network diagram. The orange colour represents the target, the orange diamond is the compound, and the green triangle is Pathway

3.5 Gene Ontology (GO) enrichment analysis

Gene Ontology (GO) enrichment analysis was conducted between the common target genes associated between *Calotropis gigantea* flowers and cervical cancer. Gene Ontology enrichment analysis revealed multiple biological processes associated with cervical cancer progression. The pathways related to responses to organic cyclic compounds, organonitrogen compounds, and oxygen-containing compounds showed the involvement of the identified targets in cellular responses to various chemical stimuli (Fig.3.5A). Additionally, some pathways were observed in cellular responses to endogenous stimuli, nitrogen-containing compounds, and chemical stress. The prominent biological pathways were related to phosphate-containing compound metabolic processes, phosphorus metabolism, and protein phosphorylation-related signalling events. Furthermore, some biological processes, such as regulation of signalling, regulation of cell communication, homeostatic processes, and stress response, were found to be enriched, highlighting the significance of coordinated signalling and adaptive cellular mechanisms in cervical cancer pathogenesis.

GO enrichment analysis of the cellular component (CC) category revealed a prominent association with cervical cancer (Fig.3.5 B). Key processes related to cellular components include membrane rafts and microdomains, which play important roles in signaling pathways and receptor-mediated interactions. Pathways involving receptor complexes, plasma membrane regions, and cell surface components suggest the crucial role of membrane-associated signalling in cervical cancer progression. Additionally, components such as extracellular vesicles, extracellular exosomes, cytoplasmic and intracellular vesicles, and cell junctions were significantly enriched, indicating the involvement of vesicle-mediated transport, intracellular communication, and cell-cell interactions. The enrichment of synapse-related structures and neuron projection-associated components shows the broader signalling and communication roles of these targets within this complex cellular network.

GO enrichment analysis of the molecular function (MF) category showed a strong correlation between functional associations and cervical cancer (Fig.3.5 C). Significant enrichments included protein serine/threonine/tyrosine kinase activity, protein serine kinase activity, and general protein kinase activity, highlighting their significant roles in kinase-mediated signalling pathways during the progression of cervical cancer. Pathways such as phosphotransferase activity, transferase activity transferring phosphorus-containing groups, and kinase binding were also involved, supporting the involvement of phosphorylation-dependent regulatory mechanisms in this process. Moreover, the enrichment of signalling receptor activity, molecular transducer activity, enzyme binding, and small-molecule binding shows the functional diversity of the identified targets in controlling signal transduction, catalytic regulation, and ligand-protein interactions associated with cervical cancer development.

6.3.6 Interpretation of KEGG Pathway Enrichment Analysis

KEGG pathway enrichment analysis showed the significant involvement of various signalling and metabolic pathways relevant to cancer progression and drug resistance (Fig.3.5 D). Steroid hormone biosynthesis is one of the most highly enriched pathways and plays a significant role in hormone-related metabolic regulation in cervical cancer. The pathway related to EGFR-tyrosine kinase inhibitor resistance involves signalling adaptation that reduces therapeutic response and increases tumour survival.

Cancer-associated pathways, such as microRNAs in cancer, pathways in cancer, and proteoglycans in cancer, were significantly enriched, showing the involvement of the identified targets in the regulation of transcription, tumour microenvironment remodelling, and oncogenic signalling processes. The enrichment of the PI3K–AKT, HIF-1, and cAMP signalling pathways highlights their involvement in survival signalling, hypoxia response, and intracellular signal transduction pathways in the pathogenesis of cervical cancer.

Inflammation and stress-related pathways, including inflammatory mediator regulation of TRP channels, AGE–RAGE signalling in diabetic complications, and chemical carcinogenesis–reactive oxygen species, involve oxidative stress, inflammatory signalling, and cellular stress responses. Additionally, pathways related to focal adhesion, calcium signalling, and neuroactive ligand–receptor interactions suggest roles in cell adhesion, migration, calcium homeostasis, and receptor-mediated communication.

Metabolic and vascular-related pathways, such as lipid and atherosclerosis, fluid shear stress and atherosclerosis, and metabolic pathways, further reveal the disruption of cellular metabolism and mechanotransduction processes.

Overall, KEGG pathway analysis showed that the identified targets are involved in diverse but interconnected pathways responsible for cell proliferation, survival, inflammation, metabolism, and therapeutic resistance, which are collectively responsible for the development and progression of cervical cancer.

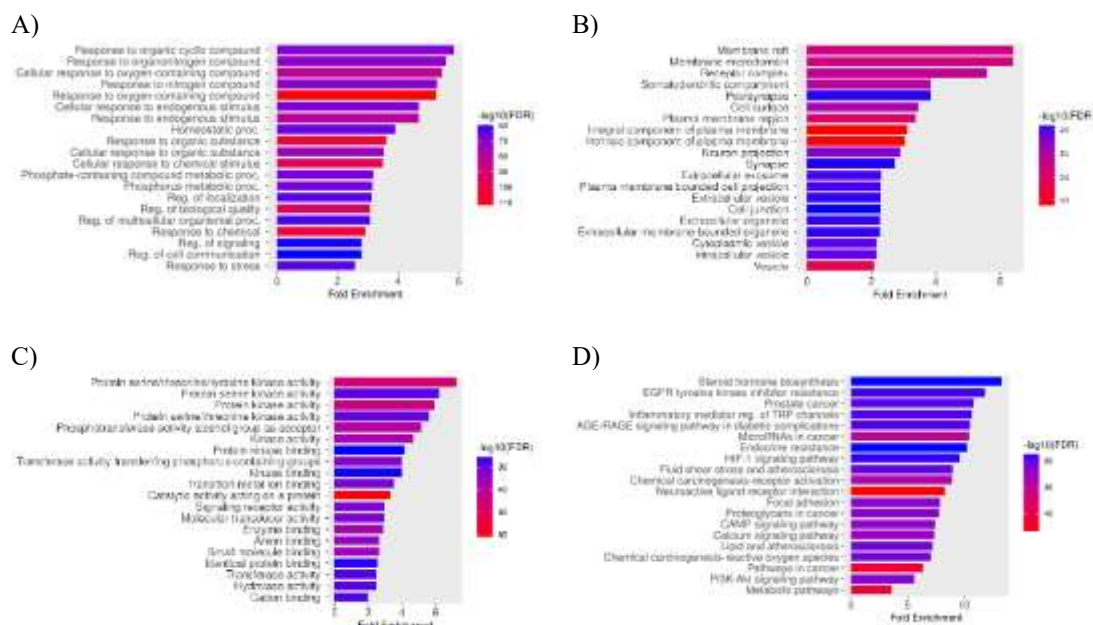


Fig. 3.5. The top 20 Gene Ontology (GO) terms pathways associated with the *Calotropis gigantea* flowers and Cervical cancer are categorized as follows: A) Biological Processes, B) Cellular Components, C) Molecular Functions, D) KEGG Pathway analysis

6.3.7 Survival Analysis

The Kaplan-Meier plotter showed that among the identified genes, JUN was significantly associated with patient outcomes, meeting the p-value threshold of 0.05 for overall survival (Fig. 3.6). Specifically, genes with high expression and their recorded associations with survival included JUN (HR = 1.7; P = 0.027), which indicated a markedly higher risk of death, and EGFR (HR = 1.6; P = 0.055), which demonstrated a borderline significant association with lower survival rates. Other genes analysed that did not reach statistical significance in their connection to survival included BCL2 (HR = 0.72; P = 0.17), AKT1 (HR = 1.1; P = 0.63), CASP3 (HR = 0.92; P = 0.74), and ESR1 (HR = 1.1; P = 0.77).

Furthermore, the results indicated that high expression of both SRC (HR = 1; P = 0.93) and STAT3 (HR = 0.99; P = 0.97) resulted in almost no difference in survival probability compared with the low expression groups. Based on these survival analyses, JUN expression at diagnosis can be considered an undesirable prognostic factor that may lower the overall survival of the studied individuals.

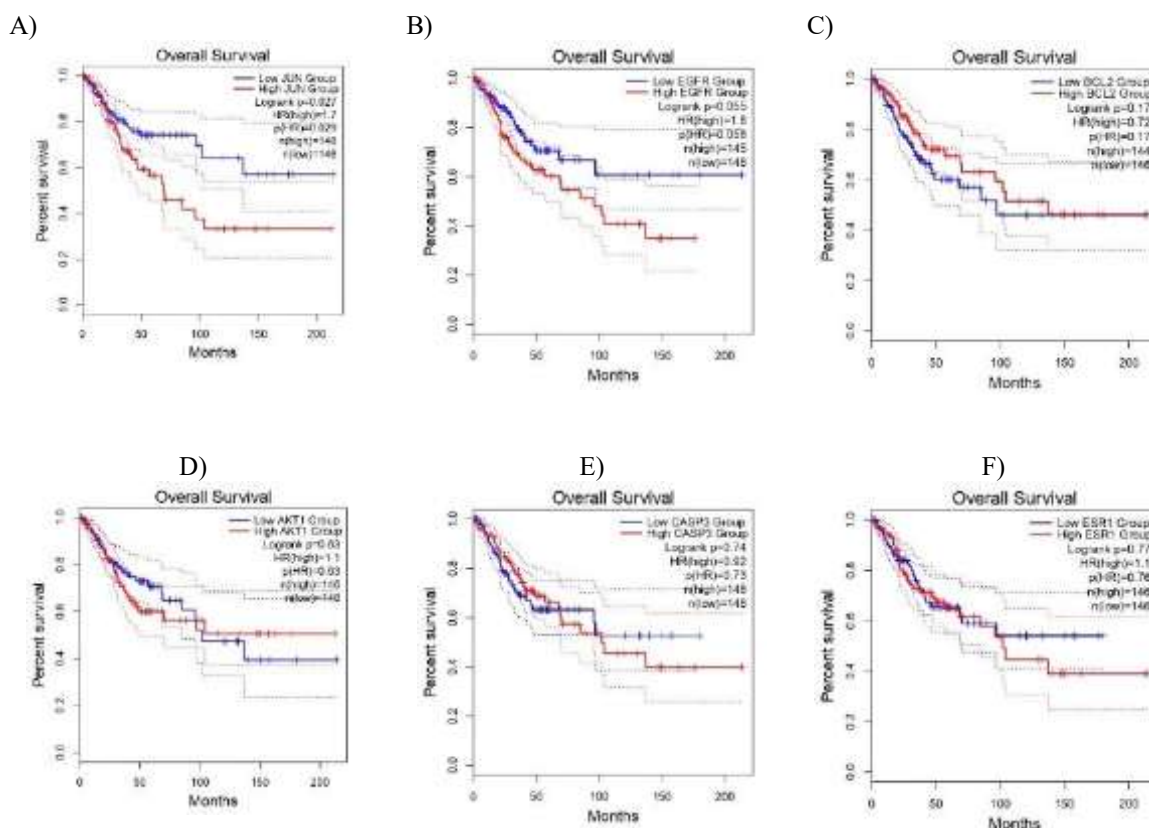


Fig. 3.6. Overall survival analyses demonstrating the prognostic significance of cervical cancer-associated hub genes were conducted using Kaplan–Meier survival curves and log-rank tests based on TCGA-CESC (cervical squamous cell carcinoma and endocervical adenocarcinoma) datasets, visualized using GEPIA2. The dashed lines indicate the upper and lower confidence intervals. (A) JUN, (B) EGFR, (C) BCL2, (D) AKT1, (E) CASP3, and (F) ESR1

3.8 Molecular Docking

Molecular docking studies were conducted to examine the binding affinities and interaction patterns of the selected bioactive compounds with key cancer-related proteins, including AKT1, EGFR, ESR1, SRC, STAT3, HSP90AA1, BCL2, and ALB. The docking results were interpreted based on binding energy, hydrogen bond interactions, and involvement of key amino acids, which together display the stability and potential biological relevance of the ligand-protein complexes, was presented in Table 3.4.

3.8.1 AKT Serine/Threonine Kinase 1-AKT1

Among the compounds docked against AKT1, quercetin and kaempferol showed strong binding affinities, with binding energies of -7.80 kcal/mol and -7.60 kcal/mol, respectively, as shown in Fig. 3.7 and Fig. 3.8. Quercetin formed several hydrogen bonds with GLU-198, GLU-228, and ALA-230, whereas kaempferol interacted with GLU-228 and ALA-230. The presence of several hydrogen bonds with key amino acid residues within the active site reflects stable ligand accommodation and signifies the role of flavonoids in modulating AKT1-mediated signalling pathways involved in cancer cell survival and proliferation

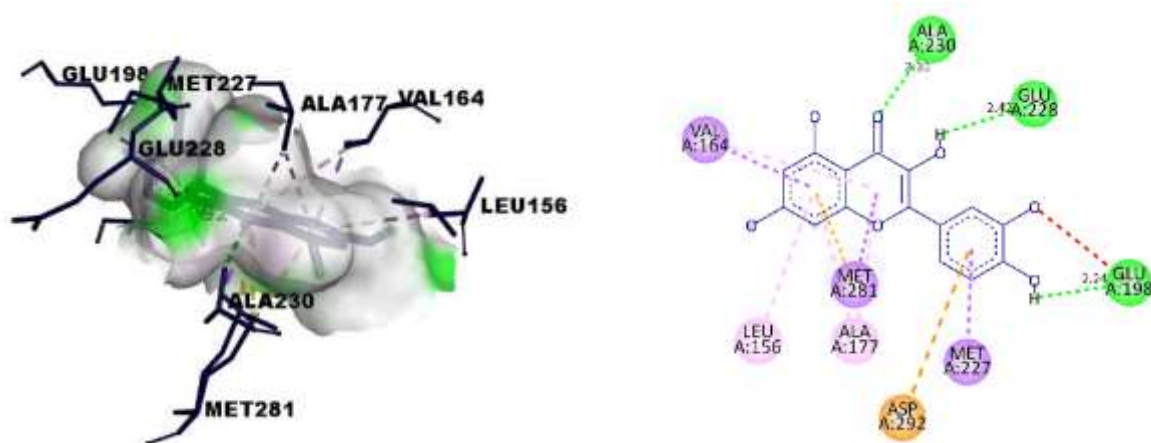


Fig. 3.7. Quercetin- AKT Serine/Threonine Kinase 1-AKT1 docked complex and interaction map

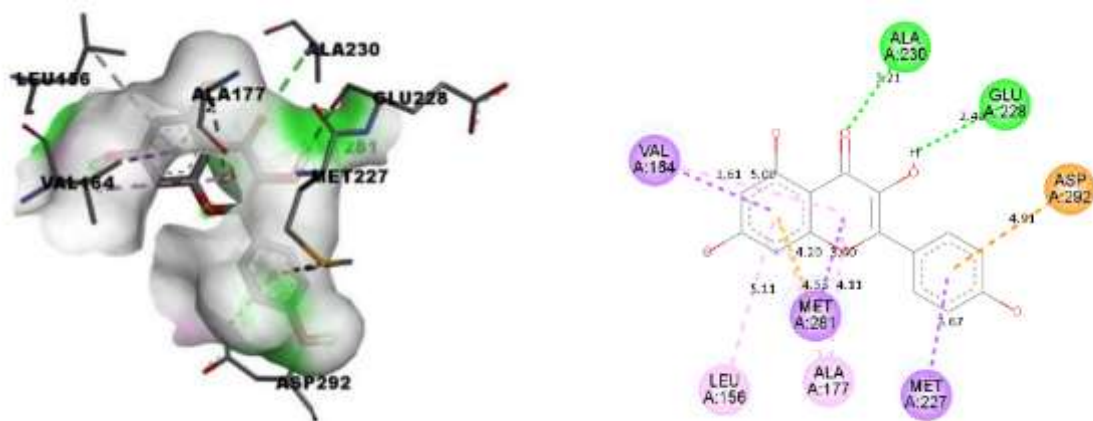


Fig. 3.8. Kaempferol-AKT Serine/Threonine Kinase 1-AKT1 docked complex and interaction map

3.8.2 Epidermal Growth Factor Receptor -EGFR

Docking against EGFR showed that quercetin (− 8.90 kcal/mol) and kaempferol (− 8.70 kcal/mol) displayed the strongest binding energies compared to the other tested bioactive compounds, as shown in Fig. 3.9 and Fig. 3.10. Both bioactive compounds interact with the critical MET-793 residue, which is essential for EGFR kinase activity. Additionally, quercetin formed hydrogen bonds with THR-854 and ASP-855, further increasing the stability of the ligand-protein complex. Notably, flavylum exhibited the lowest binding energy (−8.40 kcal/mol), despite the absence of hydrogen bond formation, indicating that hydrophobic and π - π interactions may significantly contribute to its binding affinity. These findings collectively suggest that flavonoid-based compounds are effective EGFR inhibitors.

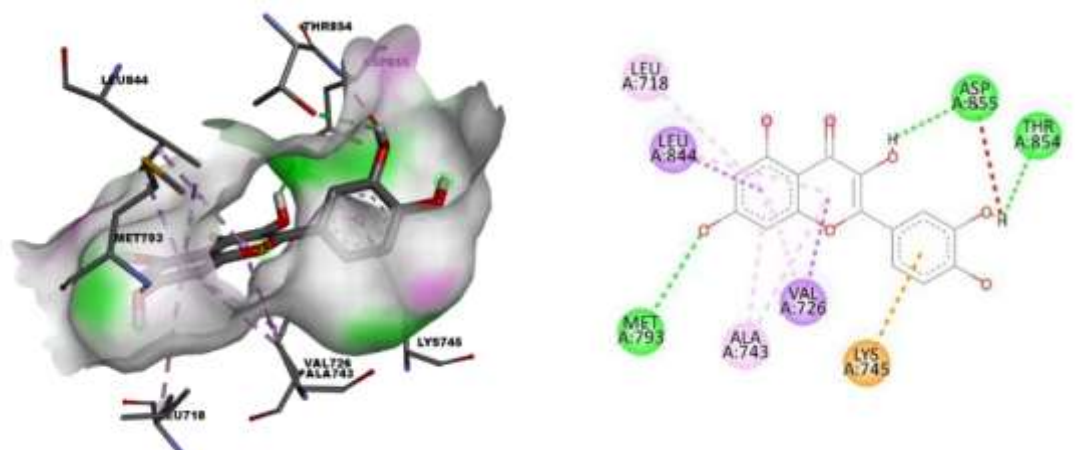


Fig. 3.9. Quercetin-EGFR docked complex and interaction map

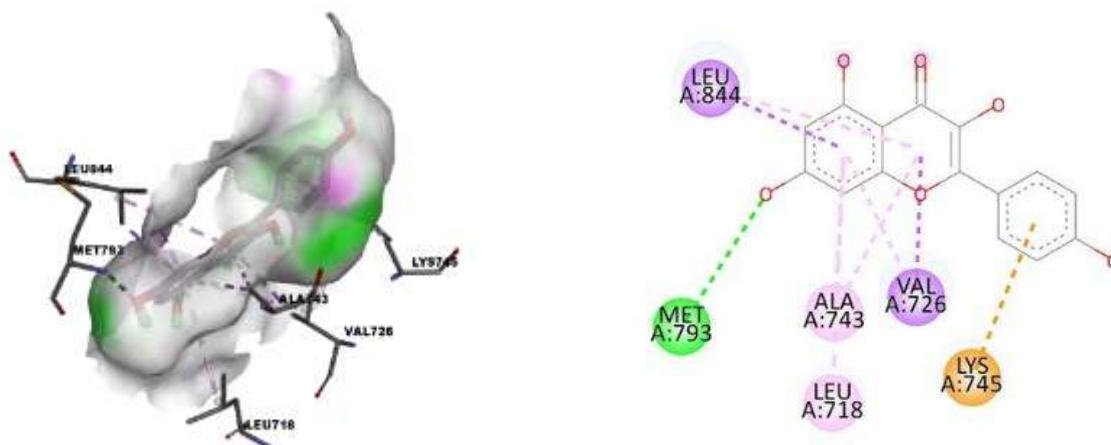


Fig. 3.10. Kaempferol- EGFR docked complex and interaction map

3.8.3 Estrogen Receptor 1-ESR1

Kaempferol and flavylum showed strong binding affinities of -8.40 kcal/mol and -8.60 kcal/mol, towards Estrogen receptor alpha (ESR1), as displayed in Fig. 3.11 and Fig. 3.12. Kaempferol develop a hydrogen bond with GLY-521, a residue involved in stabilization of ligand within the hormone-binding domain. Conversely, stigmasterol displayed weak binding affinity (-1.00 kcal/mol), poor interactions, and limited therapeutic relevance. These results indicate that the interaction between polyphenolic compounds and ESR1 potentially influences hormone-dependent cancer pathways.

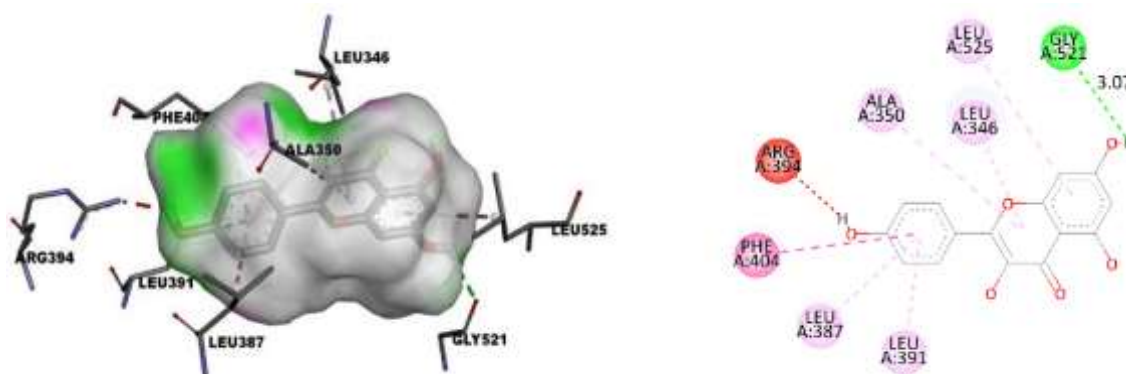


Fig. 3.11. Kaempferol- Estrogen Receptor 1-ESR1 docked complex and interaction map

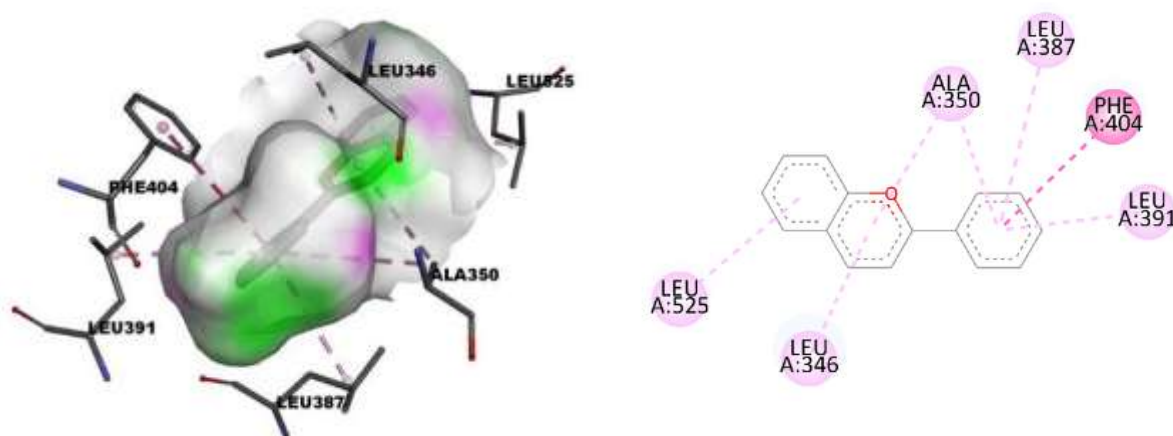


Fig. 3.12. Flavylum- Estrogen Receptor 1-ESR1 docked complex and interaction map

3.8.4 SRC Proto-Oncogene, Non-Receptor Tyrosine Kinase -SRC

Among all SRC-targeting compounds, quercetin exhibited the highest binding affinity (-9.10 kcal/mol) and formed several hydrogen bonds with LEU-273, MET-341, THR-338, and ASP-404, as shown in the Fig. 3.13. Similarly, kaempferol and taxasterol acetate displayed strong binding energies of -8.80 and -8.10 kcal/mol, respectively. The

involvement of residues such as THR-338 and MET-341, which are considered critical for SRC kinase function, suggests that these compounds effectively inhibit SRC-mediated oncogenic signalling.

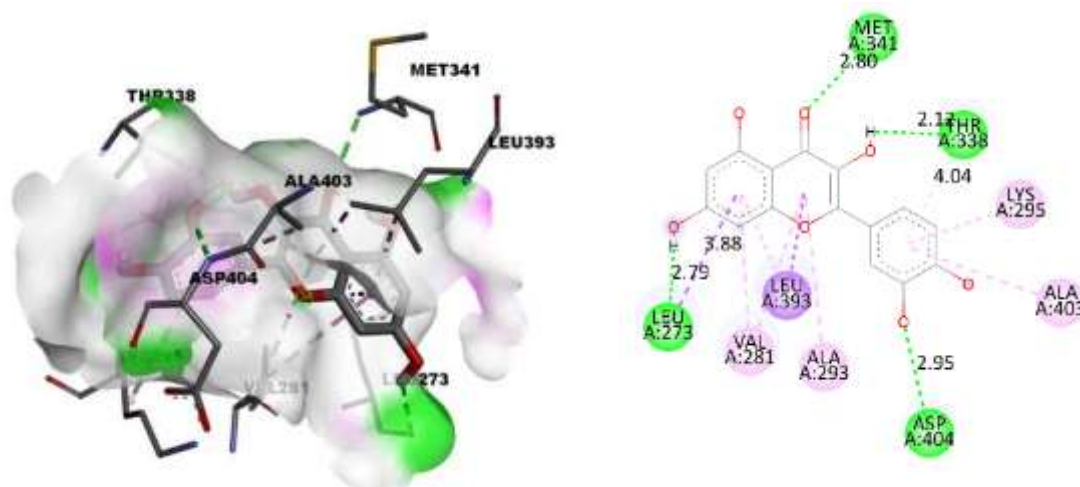


Fig. 3.13. Quercetin-SRC docked complex and interaction map

3.8.5 HSP90AA1, BCL2, and ALB

Compounds docked with HSP90AA1 and BCL2 displayed moderate binding affinities ranging from -5.00 to -5.60 kcal/mol, suggesting less dominant inhibition. Interaction with SER-52 and ASP-93 in HSP90AA1 may disrupt chaperone activity. Compounds binding to ALB show interactions rather than interacting with anticancer targets, which is consistent with its physiological role.

Overall, the molecular docking results clearly show that flavonoids, such as quercetin and kaempferol, consistently exhibit the strongest binding affinities across various cancer-relevant targets, particularly AKT1, EGFR, SRC, and ESR1. The formation of several hydrogen bonds with catalytically important residues and favourable binding energy indicates high complex stability and potential multitarget inhibitory activities. These findings demonstrate that the bioactive compounds in *C. gigantea* flowers exert anticancer effects by simultaneously modulating multiple oncogenic signalling pathways

Table 3.4: Basic information on the molecular docking results of the *Calotropis gigantea* flowers and target proteins

Molecular name	Targets	PDB ID	Residue involved in H bonding	H-bond length (Å)	Binding energy (kcal/Mol)
Kaempferol	AKT1	6CCY	ALA-230;GLU-228	3.21;2.40	-7.60
Quercetin	AKT1	6CCY	GLU-198; GLU-228;ALA-230	2.24;2.42;3.30	-7.80
9,12-Octadecadienoic acid, methyl ester	BCL2	2W3L	LEU-96	3.16	-5.60
p-(acetylamino)phenol	ALB	2BX8	ARG-257	3.05	-5.70
5-hydroxy-(2-methoxymethyl)pyridine	EGFR	1XKK	CYS-775;ASP-855;THR-854	3.82;3.69;4.33	-4.80
Acetaminophen	EGFR	1XKK	LEU-777;CYS-775	3.25;2.51	-6.20
Flavylium	EGFR	1XKK	-	-	-8.40
Glutathione	EGFR	1XKK	AL722;LYS745;ASP837;ASP855;ASN842;THR854	3.19;3.22;2.44;3.04;2.40;3.04	-6.60
Kaempferol	EGFR	1XKK	MET-793	3.26	-8.70
Quercetin	EGFR	1XKK	MET-793;THR-854;ASP-855	3.25;2.58;2.48	-8.90
Thymine	EGFR	1XKK	PHE-856	3.65	-5.20
5-hydroxy-(2-methoxymethyl)pyridine	ESR1	1X7R	-	-	-4.20
Flavylium	ESR1	1X7R	-	-	-8.60
Kaempferol	ESR1	1X7R	GLY-521	3.07	-8.40

p-(acetylamino)phenol	ESR1	1X7R	GLU-353	2.92	-6.00
Stigmasterol	ESR1	1X7R	GLU-353	2.27	-1.00
Nicotinic Acid	HSP90AA 1	1BYQ	SER-52	2.99	-5.00
p-(acetylamino)phenol	HSP90AA 1	1BYQ	SER-52;ASP-93	2.97;2.29	-5.20
5-hydroxy-(2-methoxymethyl)pyridine	SRC	2H8H	PHE-321	1.86	-4.80
9,12-Octadecadienoic acid, methyl ester	SRC	2H8H	SER-261	2.71	-6.60
Kaempferol	SRC	2H8H	THR-338;MET-341	2.61;2.82	-8.80
p-acetoaminophenol	SRC	2H8H	THR-338;PHE-405	2.98;2.92	-5.90
Quercetin	SRC	2H8H	LEU-273;MET-341;THR-338;ASP-404	2.79;2.80;2.12;2.95	-9.10
Taxasterol Acaetate	SRC	2H8H	ARG-304	2.70	-8.10
5-hydroxy-(2-methoxymethyl)pyridine	STAT3	6NJS	ARG-609;SER-611;GLU-612;SER-613	2.94;2.06;3.02;2.94	-4.00
9,12-Octadecadienoic acid, methyl ester	STAT3	6NJS	SER-611;GLU-612;SER-613	2.91;2.88;2.88	-3.30
Taxasterol Acaetate	STAT3	6NJS	SER-611;GLU-612;SER-613	2.70;2.92;3.06	-6.10
Thymine	STAT3	6NJS	ARG-445;GLU-448;SER-449	2.36;2.19;1.88	-6.10

3.9 Molecular Dynamic Stimulation Analysis

3.9.1 Molecular Dynamic Stimulation Analysis of Quercetin–SRC docked complex

In the MD simulation analysis of the Quercetin–SRC-docked complex, the main-chain deformability graph showed distinct regions of high deformability (Fig. 3.14 A). These prominent peaks indicate hinge regions, which are characteristic of flexible segments within the protein that play a major role in facilitating ligand binding. The presence of such hinge regions demonstrates the effective conformational adaptation of the target protein upon ligand binding, thereby promoting stable complex formation.

B-factor analysis revealed that the fluctuation patterns obtained from normal mode analysis (NMA) closely overlapped with those obtained from the PDB Structure (Fig. 3.14 B). The similarity in peak distribution clearly shows that ligand binding does not cause abnormal flexibility; instead, it stabilizes the intrinsic dynamic behaviour of the protein.

The eigenvalue analysis displayed a very low eigenvalue for the complex (9.14×10^{-5}), as shown in (Fig. 3.14 D). A low eigenvalue correlates with decreased energy requirements for molecular motion, signifying increased flexibility and structural adaptability of the protein. This low eigenvalue demonstrates that the protein-ligand complex is highly stable and energetically favourable, validating the strong intermolecular interactions.

The variance plot shows a relatively high cumulative variance contribution around the first few modes (Fig. 3.14 C), signifying that the collective motion governs the structural dynamics of the complex. The individual variance level was considerably high, further substantiating the presence of low-frequency motions required for biological activity and stable ligand binding.

The covariance matrix analysis displayed a balanced distribution of correlated (red), anti-correlated (blue), and non-correlated (white) motions among the residues (Fig. 3.14 E). The presence of substantial correlated and anti-correlated motions signifies effective communication between distant residues, which is crucial for the signal transduction and functional stability of the protein-ligand complex.

The Root Mean Square Fluctuation (RMSF) analysis, combined with secondary structure information, showed that most residues displayed low to moderate fluctuations, specifically within the α -helical and β -sheet regions (Fig. 3.14 G). The increased fluctuations were mainly due to the loop and coil regions, which are naturally flexible. Importantly, the residues involved in ligand binding displayed decreased fluctuations, indicating ligand-induced stabilization of the binding pocket of the target protein.

Finally, the elastic network model revealed low stiffness around the protein structures, as demonstrated by the dominance of the light grey regions (Fig. 3.14 F). This suggests that the protein can be easily deformed to accommodate ligand binding, further supporting the formation of a stable and dynamic protein–ligand complex.

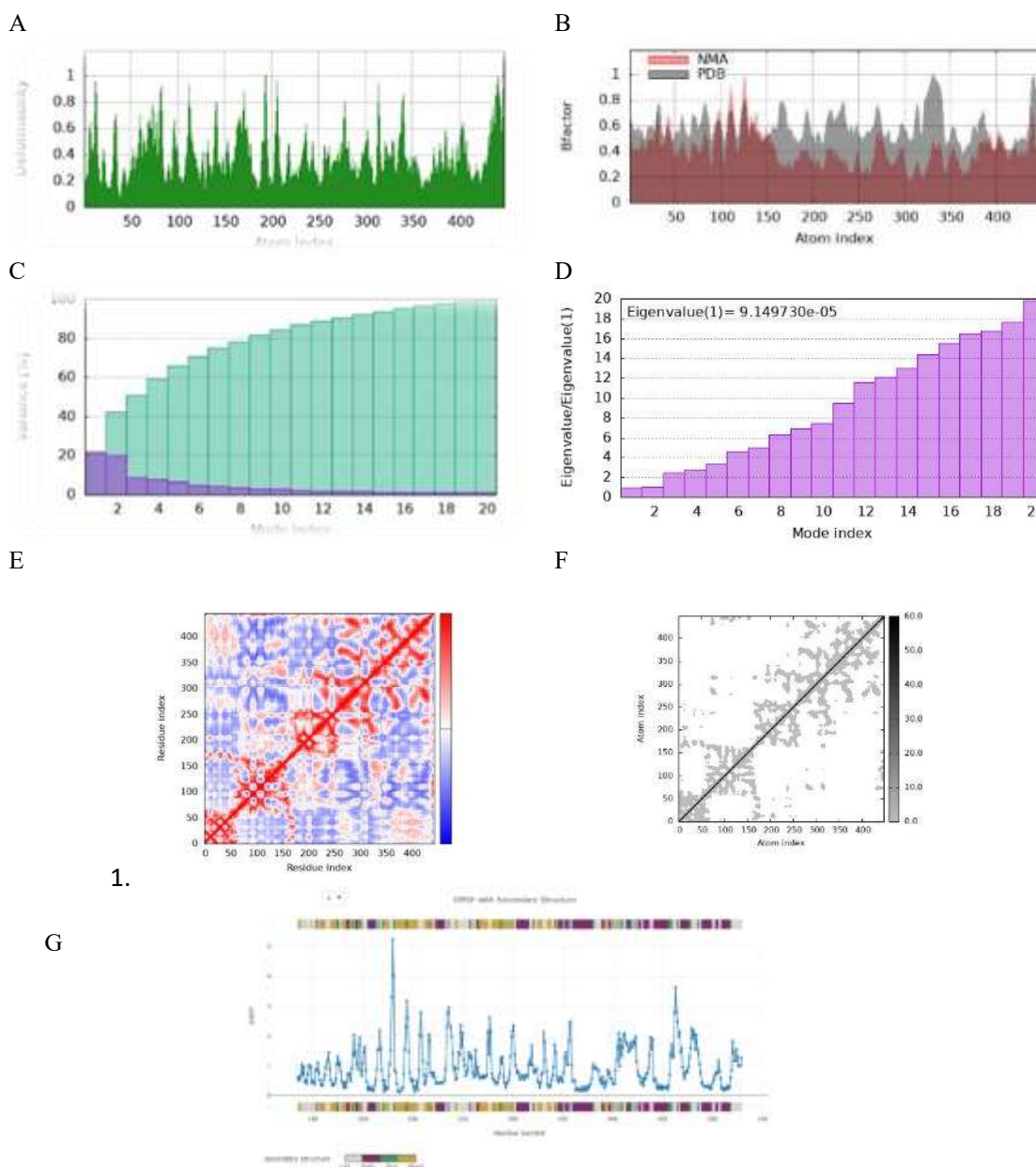


Fig. 3.14. MD simulation output for Quercetin–SRC docked complex: (A) Deformability; (B) B-factor; (C) Variance; (D) Eigenvalue; (E) Covariance map; (F) Elastic network model; (G) RMSF Analysis of the Quercetin–SRC Complex (CABS-flex 2.0) (protein rigidity: 1.0, number of cycles: 50, cycle between trajectory: 50 for 10 ns) from CABS-Flex 3.0 server

3.9.2 Molecular Dynamic Stimulation Analysis of Kaempferol–SRC docked complex

In the molecular dynamics (MD) simulation analysis of the Kaempferol–SRC-docked complex, the main chain deformability analysis showed the presence of various regions exhibiting elevated deformability (Fig. 3.15 A). These peaks are related to the hinge regions, which correspond to the flexible regions of the SRC protein that promote ligand binding and conformational adaptability of the protein. The presence of these hinge points indicates effective interactions between kaempferol and SRC, facilitating the structural adjustments required for stable complex formation.

The B-factor analysis indicated that the fluctuation patterns derived from the normal mode analysis closely aligned with those obtained from the experimental PDB structure (Fig. 3.15 B). The similarity in peak distribution indicates that ligand binding did not cause abnormal structural instability but rather maintained the intrinsic dynamic behaviour of the protein. This finding further confirms the structural integrity and stability of the kaempferol–SRC complex

The eigenvalue analysis displayed a very low eigenvalue of 9.14973×10^{-5} (Fig. 3.15 D). A low eigenvalue indicates that minimal energy is required to deform the protein structure, signifying increased flexibility and favourable conformational dynamics of the protein. This remarkably low eigenvalue demonstrates that the interaction between kaempferol and SRC is energetically favourable, leading to the formation of a highly stable protein-ligand complex.

Variance analysis showed that the cumulative variance increased constantly across the first 20 modes, with the initial modes contributing significantly to the overall motion of the complex (Fig. 3.15 C). The relatively high individual variance observed in the lower modes facilitates the dominance of collective motions, which are important for biological function and signal transduction, further confirming the dynamic stability of the kaempferol–SRC complex.

Covariance matrix analysis revealed a combination of correlated (red), anti-correlated (blue), and non-correlated (white) motions among the residues (Fig. 3.15 E). The presence of prominent correlated and anti-correlated regions indicates effective interactions between various parts of the proteins upon ligand binding. Such coordinated residue movements are indicative of functional stability and suggest that kaempferol binding activates significant dynamic responses within the SRC protein.

Root mean square fluctuation (RMSF) analysis, combined with secondary structure information, showed that most residues displayed low-to-moderate fluctuations during the simulation period (Fig. 3.15 G). Higher RMSF values were prominently observed in the loop and coil regions, which are inherently flexible, whereas the α -helical and β -sheet regions displayed decreased fluctuations. Importantly, the residues within and surrounding the ligand-binding regions showed lower RMSF values, suggesting ligand-induced stabilization of the binding pockets.

Finally, the elastic network model showed relatively low stiffness around the SRC protein structure, as indicated by the prominent light-grey regions (Fig. 3.15 F). This indicates that the protein exhibits sufficient flexibility to undergo conformational changes upon ligand binding. The low stiffness observed further supports the ability of SRC to accommodate kaempferol and the formation of a stable and flexible complex.

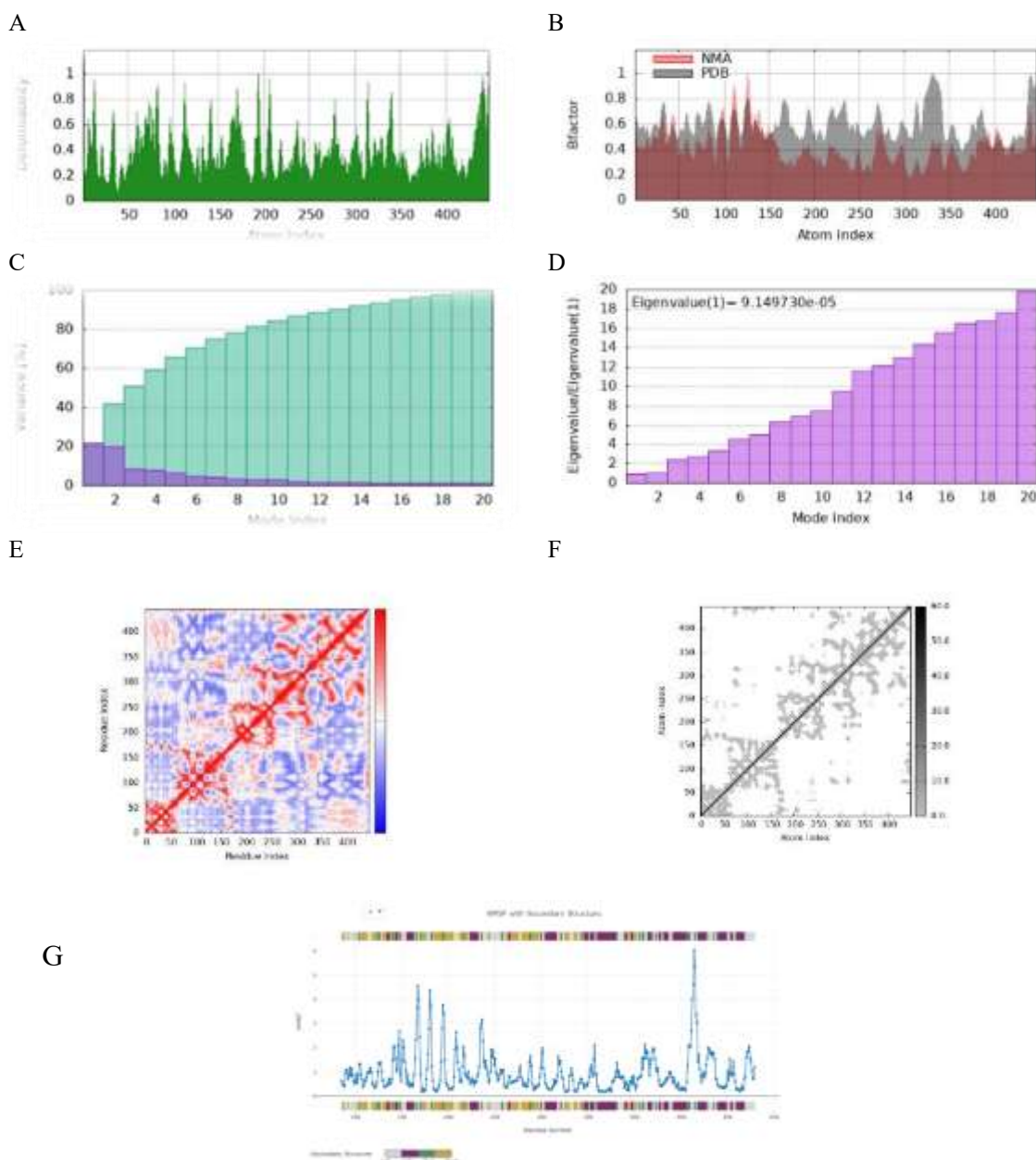


Fig. 3.15. MD simulation output for Kaempferol—SRC docked complex: (A) Deformability; (B) B-factor; (C) Variance; (D) Eigenvalue; (E) Covariance map; (F) Elastic network model; (G) RMSF Analysis of the Kaempferol—SRC Complex (CABS-flex 2.0) (protein rigidity: 1.0, number of cycles: 50, cycle between trajectory: 50 for 10 ns) from CABS-Flex 3.0 server

Discussion

The results of this study demonstrate that *Calotropis gigantea* flowers contain a diverse array of bioactive compounds that potentially exert multi-targeted anti-cervical cancer effects by modulating key oncogenic signaling pathways. By integrating network pharmacology, molecular docking, and MD simulations, we have identified specific hub genes and molecular mechanisms through which these floral bioactives may inhibit cervical cancer progression.

The phytochemical analysis of *C. gigantea* flowers identified 31 bioactive compounds, including flavonoids like quercetin and kaempferol, and cardiac glycosides such as calotropin and uscharin. ADME profiling revealed that flavonoids and small heterocyclic compounds (e.g., flavylum and 5-hydroxy-(2-methoxymethyl)pyridine) possess favorable drug-like properties, adhering to Lipinski's Rule of Five with high oral bioavailability scores (3,4). While high-molecular-weight cardenolides like uscharin and calotropin exhibited Lipinski violations due to their complexity, they remain pharmacologically significant as potent cytotoxic agents known to induce apoptosis in various cancer cell lines, including HeLa and HCT116 (16,17). This suggests that the anti-cancer potential of *C. gigantea* stems from synergistic interactions between highly bioavailable flavonoids and more complex, highly potent glycosides (11,12).

The PPI network analysis identified AKT1, EGFR, SRC, and STAT3 as critical hub genes with the highest degree of connectivity. AKT1, a central component of the PI3K-AKT pathway, is frequently mutated in cervical cancer and promotes cell survival, proliferation, and angiogenesis (6,7). Similarly, the overexpression of EGFR and SRC is closely linked to tumor growth and resistance to therapy (39,40). Our survival analysis further validated the clinical relevance of these targets, particularly JUN (HR = 1.7) and EGFR (HR = 1.6), which were identified as significant prognostic markers of poor survival in cervical cancer patients. This aligns with recent studies suggesting that targeting these core regulatory nodes can disrupt the hallmark processes of tumorigenesis (10,34).

GO and KEGG enrichment analyses provided a systems-level understanding of the "multi-component, multi-pathway" mechanism. The targets were significantly enriched in pathways such as PI3K-AKT signaling, EGFR-tyrosine kinase inhibitor resistance, and steroid hormone biosynthesis (5,8). The modulation of these pathways suggests that *C. gigantea* bioactives may not only inhibit primary tumor growth but also overcome therapeutic resistance—a major challenge in treating advanced cervical cancer (1,2). Furthermore, the enrichment of apoptosis-related terms and cell cycle control reinforce the findings that *C. gigantea* extracts induce programmed cell death by regulating pro-apoptotic factors like CASP3 and BCL2 (18,41).

Molecular docking confirmed the high affinity of flavonoids for these hub proteins. Quercetin and kaempferol consistently exhibited the strongest binding energies, particularly against SRC (−9.10 kcal/mol) and EGFR (−8.90 kcal/mol). These compounds formed stable hydrogen bonds with critical catalytic residues such as MET-793 in EGFR and THR-338/MET-341 in SRC, which are essential for kinase activity (6,9).

The MD simulations further substantiated these interactions, showing that the Quercetin—SRC and Kaempferol—SRC complexes are highly stable. The very low eigenvalues 9.14973×10^{-5} and consistent B-factor profiles indicate that the ligand-protein complexes are energetically favorable and maintain structural integrity over time (10,34). The low RMSF values in the binding residues during simulations suggest that the binding of these bioactives stabilizes the target proteins, thereby effectively inhibiting their oncogenic functions (7,42).

Conclusion

In conclusion, this study provides a comprehensive computational foundation for using *Calotropis gigantea* floral bioactives as potential therapeutic agents against cervical cancer. The integration of high-affinity binding, stable molecular dynamics, and multi-pathway modulation highlights these compounds, particularly quercetin and kaempferol, as promising candidates for further in vitro and in vivo validation.

References

- Burmeister CA, Khan SF, Schäfer G, Mbatani N, Adams T, Moodley J, et al. Cervical cancer therapies: Current challenges and future perspectives. 2022 Apr 20 [cited 2025 Nov]; Available from: <https://doi.org/10.1016/j.tvr.2022.200238>
- Caruso G, Wagar MK, Hsu H, Hoegl J, Valzacchi GMR, Fernández A, et al. Cervical cancer: a new era. 2024 Aug 8 [cited 2025 Nov]; Available from: <https://doi.org/10.1136/ijgc-2024-005579>
- Daina A, Michielin O, Zoete V. SwissADME: a free web tool to evaluate pharmacokinetics, drug-likeness and medicinal chemistry friendliness of small molecules. 2017 Mar 3 [cited 2025 Oct]; Available from: <https://doi.org/10.1038/srep42717>
- Alwin D. SwissADME. 2024 Jan 1 [cited 2025 Nov]; Available from: <https://doi.org/10.13140/rg.2.2.19938.75202>
- Ying P, Zhu Y. A network pharmacology study on the Cervix Prescription for treatment of Cervical Cancer. 2021 Aug 24 [cited 2025 Oct]; Available from: <https://doi.org/10.21203/rs.3.rs-835232/v1>

6. Kamau SW, Jepkorir M, Kipkoech G, Lagu IJL, Kanda W, Kibunja S, et al. Antiproliferative activity of *Grewia villosa* ethyl acetate extract on cervical cancer HeLa cell line: Mechanistic insights through network pharmacology and functional assays approach. 2025 Sep 24 [cited 2025 Sep]; Available from: <https://doi.org/10.1371/journal.pone.0331649>
7. Ralte L, Sailo H, Kumar R, Khiangte L, Kumar NS, Singh YT. Identification of novel AKT1 inhibitors from *Sapria himalayana* bioactive compounds using structure-based virtual screening and molecular dynamics simulations. *BMC Complementary Medicine and Therapies* [Internet]. 2024 Mar 7 [cited 2025 Oct];24(1). Available from: <https://doi.org/10.1186/s12906-024-04415-3>
8. Hasan MdT, Islam MdR, Islam MdR, Altahan BR, Ahmed K, Bui FM, et al. Systematic approach to identify therapeutic targets and functional pathways for the cervical cancer. 2023 Feb 1 [cited 2025 Oct]; Available from: <https://doi.org/10.1186/s43141-023-00469-x>
9. Butt SS, Badshah Y, Shabbir M, Rafiq M. Molecular Docking Using Chimera and Autodock Vina Software for Nonbioinformaticians. 2020 Jun 19 [cited 2026 Feb]; Available from: <https://doi.org/10.2196/14232>
10. Bhattacharya K, Nath BC, Ahmed E, Khanal P, Chanu NR, Deka S, et al. Integration of network pharmacology, molecular docking, and simulations to evaluate phytochemicals from *Drymaria cordata* against cervical cancer. 2024 Jan 1 [cited 2025 Oct]; Available from: <https://doi.org/10.1039/d3ra06297j>
11. Mutiah R, Kristanti RA, Maimunah S. Synergistic Effects of Doxorubicin and Cardenolid Glycosides of *Calotropis Gigantea* Root on Cervical Cancer Hela Cell Line. 2017 Aug 31 [cited 2025 Sep]; Available from: <https://doi.org/10.22146/tradmedj.27924>
12. Jayalekshmi C, Das NM, Periakaruppan R. Bioactive compounds of *Calotropis gigantea* for cancer treatment. 2024 Apr 5 [cited 2025 Nov]; Available from: <https://doi.org/10.1016/j.oor.2024.100336>
13. Schubert M, Bauerschlag D, Muallem MZ, Maass N, Alkatout Í. Challenges in the Diagnosis and Individualized Treatment of Cervical Cancer. *Medicina* [Internet]. 2023 May 11 [cited 2026 Feb];59(5):925. Available from: <https://doi.org/10.3390/medicina59050925>
14. Bhat SS, Sindhu R, Prasad SK. A Bioinformatics Approach Towards Plant-Based Anticancer Drug Discovery. In 2024 [cited 2025 Nov], p. 35. Available from: <https://doi.org/10.1201/9781003354437-2>
15. Gogoi B, Gogoi D, Silla Y, Kakoti BB, Bhau BS. Network pharmacology-based virtual screening of natural products from *Clerodendrum* species for identification of novel anti-cancer therapeutics. *Molecular BioSystems* [Internet]. 2016 Dec 22 [cited 2026 Jan];13(2):406. Available from: <https://doi.org/10.1039/c6mb00807k>
16. Winitchaikul T, Sawong S, Surangkul D, Srikumool M, Somran J, Pekthong D, et al. *Calotropis gigantea* stem bark extract induced apoptosis related to ROS and ATP production in colon cancer cells. *PLoS ONE* [Internet]. 2021 Aug 3 [cited 2025 Sep];16(8). Available from: <https://doi.org/10.1371/journal.pone.0254392>
17. Sawong S, Pekthong D, Suknoppakit P, Winitchaikul T, Kaewkong W, Somran J, et al. *Calotropis gigantea* stem bark extracts inhibit liver cancer induced by diethylnitrosamine. *Scientific Reports* [Internet]. 2022 Jul 15 [cited 2025 Oct];12(1). Available from: <https://doi.org/10.1038/s41598-022-16321-0>
18. Kharat KR, Kharat AS. The *Calotropis Gigantea* Methanolic Extract Induces Apoptosis in Human Breast Carcinoma Cells. *PubMed* [Internet]. 2019 Nov 1 [cited 2025 Nov];44(6):483. Available from: <https://pubmed.ncbi.nlm.nih.gov/31875083>
19. Kibushi B, Elbasyouni A, Kporde SW, Hadil S, Hussein O, Soro S, et al. Recent Advances in Alternative Medicine [Internet]. *IntechOpen eBooks*. IntechOpen; 2023 [cited 2025 Sep]. Available from: <https://doi.org/10.5772/intechopen.1000427>
20. Elbasyouni A, Kporde SW, Hussein HS, Soro O, Mulondo S, Nshimirimana J, et al. The Crosstalk between Phytotherapy and Bioinformatics in the Management of Cancer. In: *IntechOpen eBooks* [Internet]. IntechOpen; 2023 [cited 2025 Oct]. Available from: <https://doi.org/10.5772/intechopen.1001958>
21. Luo F, Gu J, Chen L, Xu X. Systems pharmacology strategies for anticancer drug discovery based on natural products. *Molecular BioSystems* [Internet]. 2014 Jan 1 [cited 2025 Nov];10(7):1912. Available from: <https://doi.org/10.1039/c4mb00105b>
22. Mohanraj K, Karthikeyan BS, Vivek-Ananth RP, Chand R, Aparna SR, Mangalapandi P, et al. IMPPAT: A curated database of Indian Medicinal Plants, Phytochemistry And Therapeutics. *Scientific Reports* [Internet]. 2018 Mar 6 [cited 2025 Aug];8(1). Available from: <https://doi.org/10.1038/s41598-018-22631-z>
23. Vivek-Ananth RP, Mohanraj K, Sahoo AK, Samal A. IMPPAT 2.0: An Enhanced and Expanded Phytochemical Atlas of Indian Medicinal Plants. *ACS Omega* [Internet]. 2023 Feb 23 [cited 2026 Mar];8(9):8827. Available from: <https://doi.org/10.1021/acsomega.3c00156>
24. Shahzadi Z, Yousaf Z, Anjum I, Bilal M, Yasin H, Aftab A, et al. Network pharmacology and molecular docking: combined computational approaches to explore the antihypertensive potential of *Fabaceae* species. *Bioresources and Bioprocessing* [Internet]. 2024 May 20 [cited 2025 Oct];11(1). Available from: <https://doi.org/10.1186/s40643-024-00764-6>
25. Sarkar K, Roy P, Panda S, Choudhuri C, Chowdhury M. Ethnomedicinal study on plant resources from sacred groves of Dakshin Dinajpur district, West Bengal, India. *Ethnobotany Research and Applications* [Internet]. 2023 Mar 13 [cited 2025 Oct];25. Available from: <https://doi.org/10.32859/era.25.32.1-35>

26. Afees OJ, Arietarhire L, Soremekun O, Olugbogi EA, Aribisala PO, Alege PE, et al. Reporting the Anti-neuroinflammatory Potential of Selected Spondias mombin Flavonoids through Network Pharmacology and Molecular Dynamics Simulations. *Research Square (Research Square)* [Internet]. 2024 Apr 11 [cited 2025 Sep]; Available from: <https://doi.org/10.21203/rs.3.rs-4248639/v1>
27. Gfeller D, Grosdidier A, Wirth M, Daina A, Michielin O, Zoete V. SwissTargetPrediction: a web server for target prediction of bioactive small molecules. *Nucleic Acids Research* [Internet]. 2014 May 3 [cited 2026 Mar];42. Available from: <https://doi.org/10.1093/nar/gku293>
28. Daina A, Michielin O, Zoete V. SwissTargetPrediction: updated data and new features for efficient prediction of protein targets of small molecules. *Nucleic Acids Research* [Internet]. 2019 May 1 [cited 2026 Mar];47. Available from: <https://doi.org/10.1093/nar/gkz382>
29. Islam MM, Sreeharsha N, Alshabrmi FM, Asif AH, Al-Dhubiab BE, Anwer MdK, et al. From seeds to survival rates: investigating *Linum usitatissimum*'s potential against ovarian cancer through network pharmacology. *Frontiers in Pharmacology* [Internet]. 2023 Oct 30 [cited 2025 Sep];14. Available from: <https://doi.org/10.3389/fphar.2023.1285258>
30. Qian K, Fu D, Jiang B, Wang Y, Tian F, Li S, et al. Mechanism of *Hedyotis Diffusa* in the Treatment of Cervical Cancer. *Frontiers in Pharmacology* [Internet]. 2021 Dec 15 [cited 2025 Oct];12. Available from: <https://doi.org/10.3389/fphar.2021.808144>
31. Janani B, Vijayakumar M, Priya K, Kim JH, Geddayy A, Shahid M, et al. A network-based pharmacological investigation to identify the mechanistic regulatory pathway of andrographolide against colorectal cancer. *Frontiers in Pharmacology* [Internet]. 2022 Aug 30 [cited 2025 Oct];13. Available from: <https://doi.org/10.3389/fphar.2022.967262>
32. pisal H, Badhe P, Mali P. Network pharmacology based virtual screening of active constituents of *moringa oleifera* and the molecular mechanism against breast cancer. *Research Square (Research Square)* [Internet]. 2024 May 22 [cited 2025 Oct]; Available from: <https://doi.org/10.21203/rs.3.rs-4452781/v1>
33. Kumar GS, Manivannan R, Nivetha B, Kamalakannan D, Bhuvaneshwari K, Ammu R, et al. Unraveling the Multi-Target Pharmacological Mechanism of *Brassica rapa* in Diabetes Treatment: Integration of Network Pharmacology and Molecular Docking Approaches. *Journal of Drug Delivery and Therapeutics* [Internet]. 2023 Apr 15 [cited 2025 Aug];13(4):13. Available from: <https://doi.org/10.22270/jddt.v13i4.5783>
34. Aarthy M, Muthuramalingam P, Ramesh M, Singh SK. Unraveling the multi-targeted curative potential of bioactive molecules against cervical cancer through integrated omics and systems pharmacology approach. *Scientific Reports* [Internet]. 2022 Aug 21 [cited 2025 Oct];12(1). Available from: <https://doi.org/10.1038/s41598-022-18358-7>
35. Wang R, Gao C, Yu M, Song J, Feng Z, Wang R, et al. Mechanistic Prediction and validation of *Brevilin A* Therapeutic Effects in Lung Cancer. *Research Square (Research Square)* [Internet]. 2024 Mar 6 [cited 2025 Sep]; Available from: <https://doi.org/10.21203/rs.3.rs-3986795/v1>
36. El-Hawary SS, Albalawi MA, Montasser AOS, Ahmed SR, Qasim S, Shati AA, et al. Network pharmacology and molecular docking study for biological pathway detection of cytotoxicity of the yellow jasmine flowers. *BMC Complementary Medicine and Therapies* [Internet]. 2023 May 20 [cited 2025 Oct];23(1). Available from: <https://doi.org/10.1186/s12906-023-03987-w>
37. Zhang D, Dong YZ, Lv J, Zhang B, Zhang X, Lin Z. Network pharmacology modeling identifies synergistic interaction of therapeutic and toxicological mechanisms for *Tripterygium hypoglaucom* Hutch. *BMC Complementary Medicine and Therapies* [Internet]. 2021 Jan 15 [cited 2025 Oct];21(1). Available from: <https://doi.org/10.1186/s12906-021-03210-8>
38. Rashid A. Untitled [Internet]. 2024 Mar [cited 2025 Nov]. Available from: <https://doi.org/10.55277/researchhub.vq5dnd6h>
39. Alblihy A. From desert flora to cancer therapy: systematic exploration of multi-pathway mechanisms using network pharmacology and molecular modeling approaches. *Frontiers in Pharmacology* [Internet]. 2024 Apr 11 [cited 2025 Oct];15. Available from: <https://doi.org/10.3389/fphar.2024.1345415>
40. Fan Z, Wang S, Xu C, Yang J, Cui B. Mechanisms of action of *Fu Fang Gang Liu* liquid in treating *condyloma acuminatum* by network pharmacology and experimental validation. *BMC Complementary Medicine and Therapies* [Internet]. 2023 Apr 20 [cited 2025 Oct];23(1). Available from: <https://doi.org/10.1186/s12906-023-03960-7>
41. Kalsoom A, Altaf A, Sarwar M, Maqbool T, Ashraf MAB, Sattar H, et al. GC-MS analysis, molecular docking, and apoptotic-based cytotoxic effect of *Caladium lindenii* Madison extracts toward the HeLa cervical cancer cell line. *Scientific Reports* [Internet]. 2024 Aug 8 [cited 2025 Aug];14(1). Available from: <https://doi.org/10.1038/s41598-024-69582-2>
42. Dua R, Bhardwaj T, Ahmad I, Somvanshi P. Investigating the potential of *Juglans regia* phytoconstituents for the treatment of cervical cancer utilizing network biology and molecular docking approach. *PLoS ONE* [Internet]. 2024 Apr 16 [cited 2025 Oct];19(4). Available from: <https://doi.org/10.1371/journal.pone.0287864>